The Journal of Molecular Diagnostics, Vol. 13, No. 6, November 2011

DOI: 10.1016/j.jmoldx.2011.07.002

Detection of *KIAA1549-BRAF* Fusion Transcripts in Formalin-Fixed Paraffin-Embedded Pediatric Low-Grade Gliomas

Yongji Tian,* Benjamin E. Rich,* Natalie Vena,*† Justin M. Craig,* Laura E. MacConaill,*‡ Veena Rajaram,§ Stewart Goldman,¶ Hala Taha,‖ Madeha Mahmoud,‖ Memet Ozek,** Aydin Sav,†† Janina A. Longtine,‡‡ Neal I. Lindeman,‡‡ Levi A. Garraway,*‡ Azra H. Ligon,*† Charles D. Stiles,§§ Sandro Santagata,¶¶‖‖ Jennifer A. Chan,¶¶ Mark W. Kieran,***††† and Keith L. Ligon*†¶¶‖‖

From the Departments of Medical Oncology, Cancer Biology,§§ and Pediatric Oncology,*** and the Centers for Molecular Oncologic Pathology,† and Cancer Genome Discovery,‡ Dana-Farber Cancer Institute, Boston, Massachusetts; the Department of Pathology and Laboratory Medicine,§ and the Division of NeuroOncology,¶ Children's Memorial Hospital, Chicago, Illinois; the Department of Pediatric Oncology and Pathology,‖ Children's Cancer Hospital, Cairo, Egypt; the Division of Pediatric Neurosurgery** and the Department of Pathology,†† Acibadem University Medical Center, Istanbul, Turkey; the Department of Pathology,‡‡ and the Division of Neuropathology,¶¶ Brigham and Women's Hospital, Boston, Massachusetts; and the Departments of Pathology,‖‖ and Pediatrics,††† Children's Hospital Boston, Boston, Massachusetts*

Alterations of *BRAF* are the most common known genetic aberrations in pediatric gliomas. They frequently are found in pilocytic astrocytomas, where genomic duplications involving *BRAF* and the poorly characterized gene *KIAA1549* create fusion proteins with constitutive B-Raf kinase activity. *BRAF* V600E point mutations are less common and generally occur in nonpilocytic tumors. The development of *BRAF* inhibitors as drugs has created an urgent need for robust clinical assays to identify activating lesions in *BRAF*. *KIAA1549-BRAF* fusion transcripts have been detected in frozen tissue, however, methods for FFPE tissue have not been reported. We developed a panel of FFPE-compatible quantitative RT-PCR assays for the most common *KIAA1549-BRAF* fusion transcripts. Application of these assays to a collection of 51 low-grade pediatric gliomas showed 97% sensitivity and 91% specificity compared with fluorescence in situ hybridization or array comparative genomic hybridization. In parallel, we assayed samples for the presence of the *BRAF* V600E mutation by PCR pyrosequencing. The data further support previous observations that these two alterations of the *BRAF, KIAA1549* fusions and V600E point mutations, are associated primarily with pilocytic astrocytomas and nonpilocytic gliomas, respectively. These results show that fusion transcripts and mutations can be detected reliably in standard FFPE specimens and may be useful for incorporation into future studies of pediatric gliomas in basic science or clinical trials. *(J Mol Diagn 2011, 13: 669–677; DOI: 10.1016/j.jmoldx.2011.07.002)*

Brain tumors are the most common solid tumors in children and are the leading cause of cancer mortality in this age group (Surveillance Epidemiology and End Results Cancer Statistics Review, *http://seer.cancer.gov/csr/1975_2006/accessed* October 21, 2010). Our understanding of the basic biology of these tumors is not well developed and resources for their diagnosis and management are limited. Most pediatric low-grade gliomas defined as World Health Organization grade I or II[1] are slow growing and have low malignant potential, but they comprise a heterogeneous group of neoplasms with diverse behaviors and somewhat unpredictable clinical outcomes. Better understanding of the molecular, cellular, and developmental biology of these tumors is needed to facilitate improvements in diagnosis and therapy.

Recent studies have highlighted the role of mutations that deregulate the activity of RAF family protein kinases leading to constitutive signaling via the mitogen-activated protein kinase pathway.[2] Most prominent of these in pediatric brain tumors is a class of genomic alterations on chromosome 7q34 that create fusions between a gene of unknown function, *KIAA1549*, and the *BRAF* gene.[3–7] As a result of these fusions, a 2-Mbp region between the two genes is duplicated in tandem such that the 5′ end of the

Supported by the Pediatric Low Grade Astrocytoma Foundation.

Accepted for publication July 6, 2011.

Current address of Y.T., Tiantan Hospital, Beijing, China; of J.A.C., Departments of Pathology and Laboratory Medicine, Oncology and Clinical Neurosciences, University of Calgary, Calgary, Alberta, Canada.

Address reprint requests to Keith Ligon, M.D., Ph.D., Department of Medical Oncology, Dana Farber Cancer Institute, 450 Brookline Ave., Boston, MA 02215. E-mail address: keith_ligon@dfci.harvard.edu.

KIAA1549 gene becomes fused with the 3′ end of *BRAF*.[6] Four single instances of similar duplications have been identified on chromosome 3 in which the *SRGAP3* gene becomes fused to the *RAF1* gene.[6–8] Three additional cases of pilocytic astrocytoma (PA) have been identified in which a 2.5-Mb deletion results in genetic fusion of *BRAF* to the *FAM131B* gene.[7] Each of these chimeric genes encodes a protein in which the C-terminal RAF kinase domain is retained intact, but the N-terminal RAF regulatory domain has been replaced by a polypeptide derived from the N-terminus of the fusion partner, *KIAA1549*, *SRGAP3*, or *FAM131B*. These fusion proteins have deregulated kinase activity that causes phosphorylation of MEK1/2[7,8] and ERK,[6,7] and can transform NIH3T3 cells.[3,7,8] The constitutive signaling is attributed to the loss of the RAF regulatory domain, and may be enhanced by membrane association of the N-terminal fusion partner domains.[6]

The junctions of these fused genes are located at diverse positions within introns such that splicing ligates exons with matching reading frames together to create functional chimeric mRNAs (Figure 2B and C, of Forshew et al[6]). Five different configurations of intronic *KIAA1549-BRAF* fusions have been identified in several studies. The distribution of these recently was reviewed by Tatevossian et al.[9] Seventy-eight percent of the reported *KIAA1549-BRAF* fusions (59 of 76) join exon 16 of *KIAA1549* to exon 9 of *BRAF* (16-9 fusion), 13% of fusions (10 of 76) connect exon 15 of *KIAA1549* to exon 9 of *BRAF* (15-9 fusion), and 7% of fusions (5 of 76) connect exon 16 of *KIAA1549* to exon 11 of *BRAF* (16-11 fusion). Single instances of two other *KIAA1549-BRAF* fusion transcripts also have been identified. They consist of *KIAA1549* exon 18:*BRAF* exon 10 (18-10 fusion) and *KIAA1549* exon 19:*BRAF* exon 9 (19-9 fusion). The *FAM131B-BRAF* fusions and *SRGAP3-RAF1* fusions are less common and more diverse in structure.[6,7]

The other *BRAF* alteration that has been found in pediatric low-grade astrocytomas is the T to A transversion at codon 600 that converts a valine to a glutamic acid (V600E), creating a highly active, constitutive kinase molecule. Activating mutations in *BRAF* are found in more than half of melanomas, about 80% of which are V600E, as well as carcinomas of the thyroid, colon, and ovary.[10,11] The V600E mutation exists in a small number of low-grade pediatric brain tumors including PAs and diffuse astrocytomas and pleomorphic xanthoastrocytomas,[4–6,12–16] a fraction of higher-grade astrocytomas (grades 3 and 4),[17] and in about half of gangliogliomas.[5,12]

Inhibitors of *BRAF*, some of which already are being evaluated in adult clinical trials, may be promising therapeutics for pediatric gliomas harboring *BRAF* V600E mutations or *BRAF* fusions.[18,19] It also is possible that *KIAA1549-BRAF* fusions contribute to other types of malignancies. As such, there is an emerging need for clinically robust technologies to identify tumors with activated forms of *BRAF* in individuals who might benefit from these targeted agents.

Because they are rare and often small in size, pediatric astrocytoma biopsy samples generally are archived only as formalin-fixed paraffin-embedded (FFPE) tissue samples in most hospitals. These FFPE tissue samples constitute a valuable resource for identifying biomarkers that may be useful for diagnosis, determining prognosis, and predicting response to treatment. The use of archival tissue samples for molecular genetic studies requires specially designed and validated assays that tolerate the degraded and fragmented nucleic acids extracted from FFPE tissues. Therefore, to better address the clinical need to identify *BRAF* mutations and to facilitate retrospective studies on archival tissue samples, we have developed and evaluated novel quantitative reverse transcribed PCR (qRT-PCR) methods for detection of multiple *KIAA1549-BRAF* fusion genes in standard FFPE samples of pediatric brain tumors. Exon–exon fusion junctions in transcripts from the hybrid *KIAA1549-BRAF* gene were detected using a panel of novel qRT-PCR assays involving short amplicons (50–100 bp). The sensitivity, specificity, and accuracy of this method were evaluated by comparison with cytogenetic data obtained with a clinical fluorescence in situ hybridization (FISH) assay and array comparative genomic hybridization (CGH). In parallel, we identified mutations at codon 600 of *BRAF* with a commercial PCR pyrosequencing method that is similarly tolerant of degraded template DNA extracted from FFPE tissue. These assays provide a new strategy for rapid and reliable evaluation of the *BRAF* status of pediatric gliomas using FFPE specimens.

Materials and Methods

Pathologic Specimens

Sections of FFPE blocks and unstained slides were obtained from the Departments of Pathology at Children's Hospital (Boston, MA), Brigham and Women's Hospital (Boston, MA), Children's Cancer Hospital (Cairo, Egypt), Children's Memorial Hospital (Chicago, IL), and Marmara University Medical Center (Istanbul, Turkey). All samples were obtained under protocols approved by institutional review boards at each institution. The FFPE specimens for which data were available had been stored as paraffin blocks at ambient temperature for up to 14 years, with an average time of 3 years. Neuropathology diagnoses were made by histologic examination according to the criteria of the World Health Organization classification[1] by three independent neuropathologists (S.S., Jennifer A. Chan, K.L.L.). PAs were subclassified further as classic (PA_c) if they had a biphasic appearance, Rosenthal fibers, and eosinophilic granular bodies, and nonclassic (PA_nc) if they lacked one or more of these specific features but still were deemed to be most closely related to PA.

RNA Isolation from FFPE and cDNA Synthesis

Specimens consisting of a total of 40-μm sections of approximately 1 cm^2 tissue in the form of unmounted scrolls or scrapings from unstained slides were obtained from each FFPE tumor specimen and placed in sterile nuclease-free microcentrifuge tubes. Paraffin was removed by extracting the tissue sections twice with 1 mL xylene. For each extraction the samples were vortexed

3 × 4 seconds, incubated for 2 minutes at room temperature, vortexed 3 × 4 seconds again, incubated for 5 minutes, and centrifuged for 2 minutes at maximum speed (12,000 to 15,000 × *g*). The supernatant was removed by aspiration. The samples then were incubated briefly in 100% ethanol followed by centrifugation to collect the tissue and the procedure was repeated with 70% ethanol. Tissue pellets were air-dried and resuspended in 200 μL lysis buffer (10 mmol/L Tris-HCL, pH 8.0; 0.1 mmol/L EDTA, 2% SDS) and 500 μg/mL of proteinase K and incubated overnight at 58°C This mixture was homogenized with an equal volume of 50% phenol, 48% chloroform, and 2% isoamyl alcohol, and was centrifuged briefly to separate the phases. The aqueous phase then was transferred to a new tube with 20 μg glycogen and 500 μL ethanol, frozen in dry ice, and centrifuged at 15,000 × *g* for 20 minutes at 4°C. The pellets were rinsed with 75% ethanol, dried briefly, and resuspended in 20 μL nuclease-free water. Samples were treated with DNase I (Roche, Indianapolis, IN) by addition of 2 μL 10× reaction buffer (Roche) and 10 units of enzyme, and incubation at 37°C for 30 minutes followed by extraction with 50% phenol, 48% chloroform, and 2% isoamyl alcohol, and precipitation with ethanol. The pellets were dissolved in nuclease-free water and stored at −80°C. RNA was quantified by UV spectrophotometry and only samples with a 260/280 ratio greater than or equal to 1.9 and a 260/230 ratio greater than or equal to 2.0 were used for analyses. cDNA was synthesized using the iScript cDNA Synthesis Kit (Bio-Rad, Hercules, CA) according to the manufacturer's protocol.

Hydrolysis Probes and qRT-PCR

Hydrolysis probe assays to detect *KIAA1549-BRAF* exon junctions were designed using the Applied Biosystems web site and were purchased from Applied Biosystems. The length of the amplicons were limited to 100 bp. The primer and probe sequences used in these assays are detailed in Table 1. The probes were labeled with fluorescent groups (5-carboxyfluorescein) at the 5′ end and proprietary minor-groove-binding nonfluorescent quenching groups at the 3′ ends. Primers were used at a final concentration of 0.9 μmol/L and probes were used at 0.25 μmol/L. Reactions (20 μL) containing cDNA from 20 ng of RNA were run in triplicate, according to the manufacturer's recommendations. Assays to detect glyceraldehyde-3-phosphate dehydrogenase (*GAPDH*) mRNA were conducted in parallel. All assays were run in separate microtiter wells. Quantitative PCR was performed using an Applied Biosystems model 7900HT machine. Reactions were first incubated at 50°C for 2 minutes, then 95°C for 10 minutes, and then for 50 cycles of 95°C for 15 seconds and 60°C for 1 minute. Fluorescence was recorded and cycles to threshold (C_T) were calculated using 7900HT Sequence Detection Software, version 2.3 (Applied Biosystems, Carlsbad, CA), as recommended by the manufacturer. Representative PCR products also were resolved on 20% polyacrylamide gels to confirm their sizes and sequenced to validate their accuracy. The utmost care was taken to ensure that amplification products did not contaminate samples to be assayed. Aside from the gel electrophoresis and sequencing procedures, all PCR plates were kept sealed and stored at −20°C or discarded after qRT-PCR. All qRT-PCR assays were repeated twice in isolated single-sample runs unless sufficient material was unavailable.

Clinical Assays

Interphase FISH was performed to detect 3′*BRAF* duplications in the Center for Molecular Oncologic Pathology of the Dana Farber Cancer Institute (Boston, MA). FISH was performed on 4-micron tissue sections using the D7Z1 DNA Probe (chromosome 7 α satellite DNA; Abbott Molecular, Abbott Park, IL) at 7p11.1-q11.1 and homebrew probes RP11-767F15 and RP11-60F17 that map to 7q34. The RP11-767F15 probe includes the 5′ region of *BRAF* and the RP11-60F17 probe includes the 3′ region of *BRAF* (unpublished data). Specimens with greater than 15% of tumor nuclei showing a hybridization pattern consistent with 3′*BRAF* duplication were designated as positive. PCR pyrosequencing assays to detect *BRAF* V600E mutations (PyroMark; Qiagen, Valencia, CA) were conducted by the Center for Advanced Molecular Diagnostics at the Brigham and Women's Hospital (Boston, MA).

Array CGH

Genomic DNA was extracted from FFPE tissues using the DNeasy Blood & Tissue Kit (Qiagen). Pooled human blood DNA (Promega, Madison, WI) was used as a reference (sex-mismatched) for all experimental samples.

Table 1. Oligonucleotides Used in qRT-PCR Assays

Assay	Primers	Specificity	Sequence	Size
16-9	Forward	*KIAA1549* exon 16	5′-GCCCAGACGGCCAACA-3′	64
	Reverse	*BRAF* exon 9	5′-CCTCCATCACCACGAAATCCTT-3′	
	Probe	16-9 junction	5′-CCCTGCAGTGACTTGAT-3′	
15-9	Forward	*KIAA1549* exon 15	5′-CGTCCACAACTCAGCCTACA-3′	68
	Reverse	*BRAF* exon 9	5′-CCTCCATCACCACGAAATCCTT-3′	
	Probe	15-9 junction	5′-TCGGATGCCCAGACTTG-3′	
16-11	Forward	*KIAA1549* exon 16	5′-GCCCAGACGGCCAACA-3′	53
	Reverse	*BRAF* exon 11	5′-ACTCGAGTCCCGTCTACCAA-3′	
	Probe	16-11 junction	5′-CCCTGCAGTAAAACAC-3′	
Hs02758991		*GAPDH* exons 7 and 8	Proprietary	93

DNA was chemically labeled using the Genomic DNA ULS Labeling Kit (Agilent Technologies, Palo Alto, CA) according to the manufacturer's recommendations. Tumor and reference DNA samples (2 μg each) were labeled separately using Cy5 and Cy3 dyes, respectively, and hybridized to SurePrint G3 Human CGH 1 × 1M microarrays (Agilent Technologies, Palo Alto, CA) for 40 hours at 65°C. Microarrays were washed as specified by the manufacturer and scanned on an Agilent DNA microarray scanner. Images were analyzed and $\log_2$ ratios of signal intensities were obtained using Agilent Feature Extraction software (version 10.5). Data analysis was performed using the Agilent Genomic Workbench software suite using the Aberration Detection Method 2 algorithm with a threshold of 6.0. For algorithm analyses, the aberration filter settings were adjusted to detect aberrant segments containing a minimum of 5 probes, and the log ratio cut-off value was set to an average log ratio greater than 0.35. *BRAF* duplications were identified by a region of single-copy gain between the *KIAA1549* (138 Mbp) and *BRAF* (140 Mbp) genes on chromosome 7.

Calculation of Specificity, Sensitivity, and Concordance

Results were classified as true positive (TP), true negative (TN), false positive (FP), or false negative (FN). Specificity was calculated as TN/(TN + FP). Sensitivity was calculated as TP/(TP + FN). Concordance was calculated as (TN + TP)/(TN + TP + FN + FP). Confidence intervals were computed using a web calculator (*http://faculty.vassar.edu/lowry/clin1.html*, last accessed June 30, 2011).

Results

Detection of KIAA1549-BRAF *Fusion mRNAs in FFPE Samples*

The breakpoints that form the fusion junctions between the *KIAA1549* and *BRAF* genes are found at diverse positions within introns that range from 1.3 to 8.9 kb in size. Therefore, it is impractical to develop simple assays to identify the diverse junctions in DNA extracted from FFPE tissue. However, the fusion genes produce accurately spliced fusion mRNAs, making RNA-based assays highly specific. To more reliably detect *KIAA1549-BRAF* fusion transcripts in FFPE samples, we devised hydrolysis probe qRT-PCR assays, which exploit the 5′−3′ exonuclease activity of Taq polymerase,[20] to detect the three most common fusion junctions: 16-9, 15-9, and 16-11. These assays are particularly suited to the analysis of RNA from FFPE tissues because they involve amplification of small targets, in the 50- to 100-bp range. The scheme of these assays is displayed in Figure 1. For each assay one amplifying primer is complementary to the *KIAA1549* exon sequence, the other amplifying primer is complementary to the *BRAF* exon sequence, and the probe oligonucleotides span the junction of the fused exons. For all samples, fusion-specific assays were conducted in parallel with assays for *GAPDH* to control for the quantity and quality of the RNA in the sample preparations. The 93-bp fragment amplified in the *GAPDH* assay is the longest amplicon of all of the assays.

The specific sequences of the amplification and probe oligonucleotides used in the novel assays and the name of the proprietary *GAPDH* assay used in this study are presented in Table 1, along with the sizes of the amplicons for each assay. *KIAA1549-BRAF* fusion transcripts were reliably detected in samples with duplications of the *BRAF* gene. Amplicons were not detected in specimens lacking the duplication. Each of the junction-specific assays was applied to samples of ovarian carcinoma, thyroid carcinoma, colon carcinoma, melanoma, and mouse brain. Although *GAPDH* was detected, no fusion junctions were detected in any of these (not shown). The assay was judged to have technically failed for the single specimen in which *GAPDH* was not detected (IST-052).

Figure 2 depicts typical results of qRT-PCR experiments. Fusion-specific junctions were not detected in cDNA prepared from most samples in which duplications of the *BRAF* gene were not detected by the validation methods of FISH or CGH (Figure 2A). The 16-9 fusion junction was detected in 28 of the 32 samples in which *BRAF* duplications were identified by interphase FISH (Figure 2B). The 15-9 and 16-11 fusion junctions (2 of each) were detected in the remaining four samples in

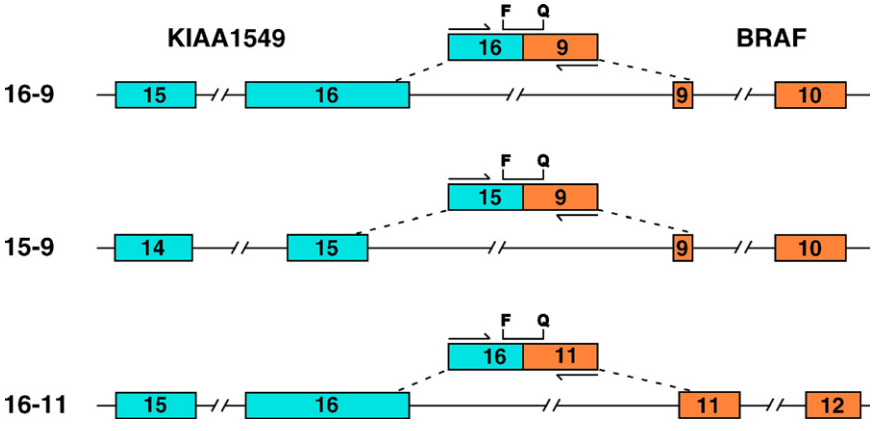

Figure 1. Design of qRT-PCR assays for detection of *KIAA1549-BRAF* fusions in FFPE samples. Select exons of the human *KIAA1549* (blue) and *BRAF* (orange) genes are depicted to illustrate the configuration of the three most common fusion transcripts and the qRT-PCR assays developed to detect them. The positions of the amplification primers (**arrows**) and the probes for each fusion are indicated. Probe sequences are unique to each transcript. Sequences of primers and probes are detailed in Table 1. F, reporter fluorophore; Q, minor groove binding quencher.

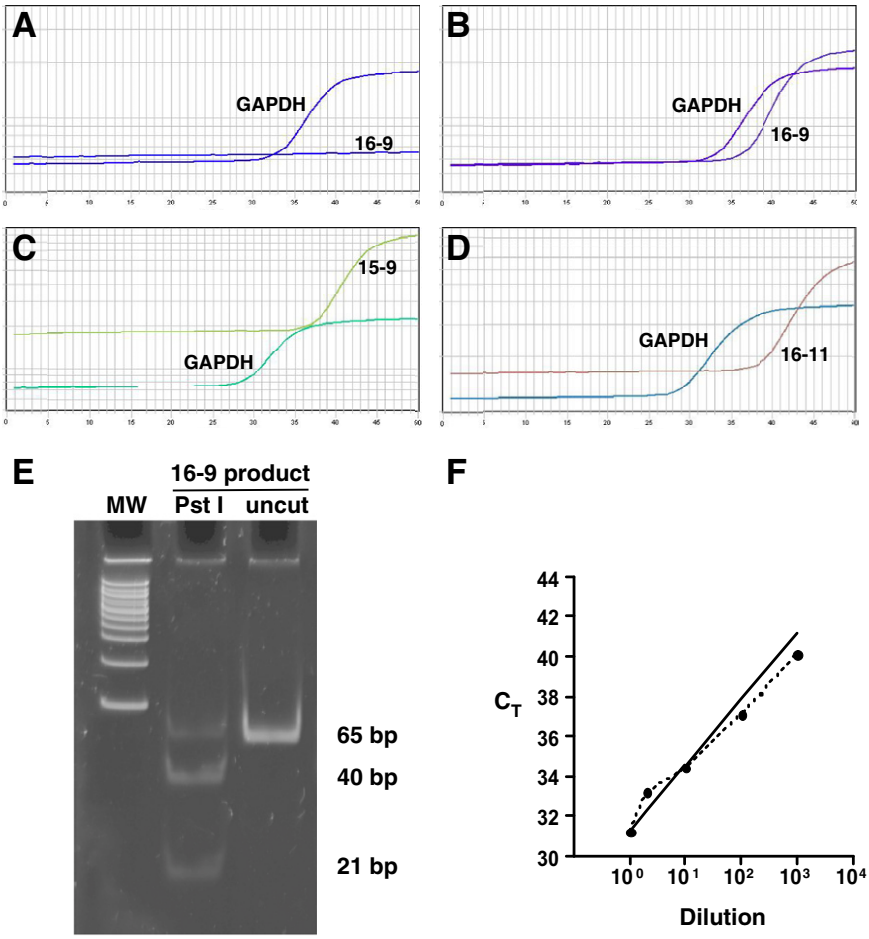

Figure 2. Representative results of *KIAA1549-BRAF* fusion detection by qRT-PCR in FFPE glioma samples. Real-time qRT-PCR assays for the fusions 16-9, 15-9, and 16-11 were compared with the positive control *GAPDH*. **A:** Negative result for 16-9 *BRAF* fusion in a pilocytic astrocytoma lacking *BRAF* duplication. Positive assay results for 16-9 (**B**), 15-9 (**C**) and 16-11 (**D**) *BRAF* fusions as detected in pilocytic astrocytomas with *BRAF* fusions validated by FISH or CGH. Traces indicate fluorescence (*y* axis) versus reaction cycles (*x* axis). **E:** Digestion of the 16-9 assay product with PstI shows appropriately sized fragments confirming specificity. **F:** Serial dilution of 16-9 positive tumor cDNA sample with benign tissue cDNA shows the linear detection range of the assay. C_T values (*y* axis) are plotted against the percentage of the 16-9 positive sample (*x* axis). The theoretical relationship between dilution and C_T in a 100% efficient reaction is plotted as a solid line. The observed values are displayed as filled circles connected by a dotted line.

which *BRAF* duplications were identified by FISH (Figure 2, C and D). The median C_T value for *GAPDH* assays was 31.34; the median C_T value for 16-9 fusion assays was 38.97; the median C_T value for 15-9 fusion assays was 39.64; and the median C_T value for 16-11 fusion assays was 36.38.

To confirm that the sequences amplified in the fusion junction qRT-PCR reactions are correct, representative reaction products were sequenced. The 16-9 amplification product was also characterized by polyacrylamide gel electrophoresis (Figure 2E). The sizes of the amplification product and PstI digestion products are consistent with the predicted molecular weights. To evaluate the efficiency of the qRT-PCR reactions we serially diluted cDNA from specimens containing fusion products diluted into cDNA from a benign brain specimen collected during epilepsy surgery. Figure 2F depicts a representative plot of C_T versus dilution. The close approximation of the experimental values to the theoretical optimum shows the dynamic range of the assay.

Similar assays were prepared to detect 18-10 and 19-9 fusion junctions and were applied to all of the samples for which *BRAF* duplications were detected by interphase FISH. No 18-10 or 19-9 fusion junctions were detected in any of the samples analyzed in this study (data not shown), consistent with the reported rarity of these events.

Detection of Fused mRNAs Correlates with BRAF *Duplication in Samples from Diverse Institutions*

There is significant variability in the quantity and quality of RNA extracted from FFPE tissue samples from different clinical laboratories at different times. Therefore, it is important to examine the effectiveness of assays with the potential for clinical use on samples from different sources. To do this a panel of 71 FFPE clinical samples was assembled from five institutions: Children's Hospital Boston (Boston, MA), Children's Cancer Hospital (Egypt), Marmara University Medical Center (Istanbul, Turkey), Children's Memorial Hospital (Chicago, IL), and Brigham and Women's Hospital (Boston, MA). The specimens had been stored as paraffin blocks at ambient temperatures from 1 week to 14 years. Forty-one of the samples were diagnosed as PA. These included 30 PA_c, 7 that were diagnosed as PA_nc, and 4 additional tumors for which PA was part of a differential diagnosis. Thirty of the samples were not PA. These included 15 specimens of adult glioblastoma multiforme (GBM), 8 of ganglioglioma (GG), 1 diffuse grade 2 astrocytoma (A2), 1 low-grade glioma not otherwise specified (LG_nos), and 5 specimens of non-neoplastic brain resected in the course of surgi-

Table 2. Summary of Cases

Diagnosis	Total number of cases	*BRAF* duplications by FISH	*BRAF* duplications by CGH	*KIAA1549 BRAF* fusions by qRT-PCR	*BRAF* V600E mutations
PA_c	30	24/28	5/5	27/29	0/15
PA_nc*	11	8/9	ND	8/11	0/8
GG	8	0/7	ND	0/8	6/8
Adult GBM	15	0/2	0/6	0/15	0/6
Epilepsy	5	nd	ND	0/5	ND
A2	1	0/1	ND	0/1	ND
LG_nos	1	0/1	ND	0/1	ND

*PA_nc includes 3 samples for which PA_nc is part of a differential diagnosis (see Table 3).
ND, not done.

cal treatment for epilepsy. The specific samples and results are summarized in Table 2 and detailed in Table 3.

Each of the specimens in the PA group and 15 of the specimens in the non-PA group were assayed for *BRAF* duplication by interphase FISH. *BRAF* was found to be duplicated in 32 of the PA specimens and not duplicated in 5 specimens. None of the 11 non-PA specimens for which FISH was technically successful were found to have *BRAF* duplication. Four of the PA group specimens and four of the non-PA specimens failed to yield satisfactory data with the FISH assay. Six of the GBM were examined previously by CGH and no increases in copy number were found in the interval between *BRAF* and *KIAA1549* (data not shown).

RNA was extracted from each of these specimens and cDNA was prepared. Each cDNA sample was tested with the qRT-PCR assays to detect the three exon-specific *KIAA1549-BRAF* fusion junctions, as well as *GAPDH*. In 70 of 71 samples *GAPDH* was detected at a level high enough ($C_T < 40$) such that the fusion junctions could be identified reliably. The results of these assays are summarized in Table 2. Fusion junctions were identified in 31 of the 32 PA group samples in which *BRAF* duplication was detected by interphase FISH. Fusion junctions also were detected in two of the five samples that were found not to have duplicated *BRAF* by FISH. Of the four samples that could not be assessed by FISH, two were found to have fusion junctions, one was found not to have fusion junctions, and one failed qRT-PCR (noted earlier). It is noteworthy that two different fusion junctions were detected in four samples. No fusion junctions were detected in any of the 30 non-PA samples.

Duplications of BRAF *and Point Mutations in Codon 600 Appear Not to Overlap*

In previous studies, about half of GGs were found to have the activating *BRAF* V600E mutation.[5,12] It is therefore of interest to examine the relationship between *BRAF* missense mutations and duplications in this group of specimens. Thirty of the PA group and 15 of the non-PA group, including all of the GGs, were subjected to PCR pyrosequencing analysis to detect mutations at codon 600 of *BRAF*. V600E mutations were found in six of the eight GGs and in no other specimens. Seven of these specimens were described previously, five of which have the V600E mutation.[12] In each case the PCR pyrosequencing results are in agreement with the previous results obtained with mass spectrometry.

The Panel of qRT-PCR Fusion Junction Reactions Is a Sensitive and Specific Assay to Detect BRAF *Duplication Events*

The purpose of developing this panel of novel qRT-PCR assays was to provide a highly sensitive and specific method for detecting *BRAF* fusion/duplication events that is rapid, cost effective, and widely applicable. To gauge the effectiveness of the assays, the results of FISH assays and array CGH data were taken as true and each result was categorized as TP, TN, FP, or FN (Table 3). The sensitivity of the assay to detect *BRAF* duplications is as follows: $31/(31 + 1) = 97\%$. The 95% confidence interval for the sensitivity of the assay is 82% to 100%. The specificity of the assay to detect *BRAF* duplications is as follows: $21/(21 + 2) = 91\%$. The 95% confidence interval for the specificity is 70% to 98%. The overall concordance of the assay to detect *BRAF* duplications is 95%.

Discussion

The focal duplication on chromosome 7, resulting in the fusion of the catalytic domain of *BRAF* to part of the *KIAA1549* gene, appears to be a critical event in the formation of most if not all pilocytic astrocytomas. Thus, the evidence so far suggests that this mutation may be a useful or, possibly, defining feature for diagnosis of these tumors. In addition, constitutive signaling by the encoded chimeric protein appears to drive the inappropriate growth of these cells and hence could provide an opportunity for targeted therapeutic intervention.

A number of selective inhibitors of wild-type and mutant forms of *BRAF* are being developed as therapeutic agents for melanoma and other malignancies involving deregulated *BRAF*. Some of these ultimately might be useful for the management of low-grade astrocytomas but likely would be considered only in patients whose tumors are prospectively known to harbor the mutation. Therefore, it is important to develop and implement assays to detect fusions between the *KIAA1549* and *BRAF* genes that are both sensitive and reliable for clinical practice. Although the specific junctions in genomic DNA

Table 3. Samples Used in Study

Sample	Diagnosis	*BRAF* Duplication	Method	Notes	*BRAF* Fusion qRT-PCR	*BRAF* Codon 600	Duplication Detection
BOS-001	PA_c	YES	FISH	focal duplication	16-9, 15-9	fail	true positive
BOS-004	PA_c	YES	FISH		16-9	wild type	true positive
BOS-006	PA_c	YES	FISH		16-9	wild type	true positive
CAI-003	PA_c	YES	FISH		16-9	ND	true positive
CAI-008	PA_c	NO	FISH	11% duplicated	16-9	ND	false positive
CAI-009	PA_c	YES	FISH		16-9	ND	true positive
CAI-010	PA_c	YES	FISH		16-9, 15-9	ND	true positive
CAI-038	PA_c	YES	FISH		16-9	ND	true positive
CAI-066	PA_c	YES	FISH		16-9	ND	true positive
CAI-072	PA_c	YES	FISH		16-9	ND	true positive
CAI-073	PA_c	YES	FISH		16-9	ND	true positive
CMH-027	PA_c	YES	FISH		16-9	ND	true positive
IST-011	PA_c	YES	FISH		16-9	wild type	true positive
IST-015	PA_c	fail	FISH	looks duplicated	16-9	wild type	
IST-017	PA_c	NO	FISH		NONE	wild type	true negative
IST-018	PA_c	NO	FISH		NONE	wild type	true negative
IST-019	PA_c	NO	FISH	8% duplicated	16-9, 16-11	fail	false positive
IST-022	PA_c	YES	FISH		16-9	wild type	true positive
IST-023	PA_c	YES	FISH		16-9	fail	true positive
IST-033	PA_c	YES	FISH		15-9	fail	true positive
IST-037	PA_c	YES	FISH		16-9	wild type	true positive
IST-051	PA_c	YES	FISH		16-9	wild type	true positive
IST-052	PA_c	fail	FISH		FAIL	ND	
LGG-073	PA_c	YES	FISH & CGH		16-9	wild type	true positive
LGG-091	PA_c	YES	FISH & CGH		16-9	wild type	true positive
LGG-107	PA_c	YES	FISH & CGH		16-9	wild type	true positive
LGG-172	PA_c	YES	FISH & CGH		16-9	wild type	true positive
LGG-198	PA_c	YES	FISH		16-11	wild type	true positive
LGG-200	PA_c	YES	FISH & CGH		16-9	wild type	true positive
IST-003	PA_c	YES	FISH		16-9	fail	true positive
BOS-002	PA_nc	fail	FISH		16-9	wild type	
IST-006	PA_nc	YES	FISH		NONE	fail	false negative
IST-013	PA_nc	YES	FISH		15-9	wild type	true positive
IST-025	PA_nc	YES	FISH		16-9	wild type	true positive
IST-032	PA_nc	YES	FISH		16-9	wild type	true positive
IST-034	PA_nc	NO	FISH		NONE	wild type	true negative
LGG-137	PA_nc	YES	FISH		16-9	wild type	true positive
BOS-007	PA_nc	YES	FISH		16-11	wild type	true positive
IST-020	PA_nc v. A2	YES	FISH		16-9	wild type	true positive
IST-009	PA_nc v GG_c	fail	FISH		NONE	fail	
CMH-010	PA_nc v LG_nos	YES	FISH		16-9, 15-9		true positive
LGG-058	LG_nos	NO	FISH		NONE	wild type	true negative
BOS-003	GG_c	NO	FISH		NONE	V600E	true negative
LGG-097	GG_c	NO	FISH		NONE	V600E	true negative
LGG-100	GG_c	NO	FISH		NONE	wild type	true negative
LGG-202	GG_c	NO	FISH		NONE	wild type	true negative
LGG-267	GG_c	NO	FISH		NONE	V600E	true negative
LGG-285	GG_c	NO	FISH		NONE	V600E	true negative
BOS-023	GG_c	NO	FISH		NONE	V600E	true negative
LGG-132	GG_nc	NO	FISH		NONE	V600E	true negative
BOS-005	GBM	fail	FISH		NONE	wild type	
BOS-009	GBM	fail	FISH		NONE	wild type	
BOS-010	GBM	fail	FISH		NONE	wild type	
BOS-011	GBM	NO	FISH		NONE	wild type	true negative
BOS-012	GBM	fail	FISH		NONE	wild type	
BOS-013	GBM	NO	FISH		NONE	wild type	true negative
BOS-014	GBM	ND			NONE	ND	
BOS-015	GBM	NO	CGH		NONE	ND	true negative
BOS-016	GBM	NO	CGH		NONE	ND	true negative
BOS-017	GBM	NO	CGH		NONE	ND	true negative
BOS-018	GBM	NO	CGH		NONE	ND	true negative
BOS-019	GBM	NO	CGH		NONE	ND	true negative
BOS-020	GBM	NO	CGH		NONE	ND	true negative
BOS-021	GBM	ND			NONE	ND	
BOS-022	GBM	ND			NONE	ND	
CAI-075	A2	NO	FISH		NONE	ND	true negative
BOS-024	seizure	ND			NONE	ND	
BOS-025	seizure	ND			NONE	ND	
BOS-026	seizure	ND			NONE	ND	
BOS-027	seizure	ND			NONE	ND	
BOS-029	seizure	ND			NONE	ND	
MUS-001	Mouse brain	ND			NONE	ND	
MUS-002	Mouse brain	ND			NONE	ND	

ND, not done.

formed by these fusions are diverse, the processed mRNAs from the fused genes occur in a small number of configurations. To take advantage of this we have created a panel of highly sensitive assays to detect each of the five splice junctions known to arise in *KIAA1549-BRAF* fusion mRNAs. The two rarest of these junctions, 18-10 and 19-9, have each been identified only once in the 76 specimens reported in published studies.[9] Neither of these rare junctions was detected in this cohort of 40 samples with pilocytic features.

Although most of the pilocytic samples were diagnosed as PA_c or PA_nc, four samples had PA_nc as part of a differential diagnosis but could not be subclassified further. In three of these samples, *BRAF* was duplicated and fusion junctions were detected. Having this contributory genetic evidence in a clinical setting would allow neuropathologists and neuro-oncologists to consider these tumors as being more likely consistent with PA. The fourth of these samples was diagnosed as PA_nc or GG. FISH and *BRAF* pyrosequencing both failed, likely technically owing to the low quality of nucleic acids extracted from this sample. *GAPDH* amplicons were detected, however, and fusion junctions were absent, illustrating that the qRT-PCR fusion-junction assay may be more robust and sensitive than FISH and pyrosequencing. In this setting, the qRT-PCR assay then would provide genetic support that this tumor is less likely to represent a pilocytic tumor.

Of the 54 samples for which the presence or absence of *BRAF* duplication was determined by interphase FISH or array CGH, there were only three in which the detection of fusion junctions by PCR was discrepant with the FISH duplication status. In two of these, fusion junctions were detected by FISH, but the samples were interpreted as being not duplicated because they had *BRAF* duplications in 11% and 8% of nuclei. A threshold of 15%, established by evaluation of normal tissue, is used as a minimum for determining duplication by FISH. These discrepancies therefore may reflect focal or heterogeneous tumor pathology. The third sample was determined to have a *BRAF* duplication by FISH analysis but no junctions were detected by qRT-PCR. There are several possible reasons for this. Because *GAPDH* is expressed at a higher level than the *KIAA1549-BRAF* fusion transcripts, it is possible that the quality of the RNA in this sample was such that *GAPDH* was detectable whereas existing fusion transcripts were not detectable. Another possibility is that this specimen contains an 18-10 or 19-9 fusion, but the assay we devised that is specific for this junction is not sufficiently optimized. It also is possible that the duplication involves some other fusion that has not been identified previously. Further studies will need to be performed to distinguish between these possibilities.

Fusions between *KIAA* and *BRAF* in PA_c previously were shown to be somatic in origin and absent from matched nonmalignant tissue (blood).[3] Matched blood generally was not available for the cohort of samples in this study, but most FISH analyses include nonmalignant cells in which duplication of the 3′ end of the *BRAF* gene is uniformly absent (not shown).

One of the novel findings in our study was that some individual tumors appeared to express more than one type of gene fusion mRNA. Of the 35 tumors in which *KIAA1549-BRAF* fusion junctions were detected, four (11%) contained two different fusion transcripts. The predominant 16-9 junction is present in each of these, but three were found to also have the 15-9 junction and another one had the 16-11 junction. The mechanism and significance of these multiple fusion events are unclear. The possibility of cross-contamination must be considered; however, in the three cases for which sufficient material was available, the results were reproduced in isolated single-sample assays.

FISH analyses showed that two of these tumors had a distinct population of cells with trisomy 7 of the duplicated alleles (10% and 14%, respectively), raising the possibility that two different duplication alleles were created by separate events. However, the other two samples with two different fusions had very little or no trisomy ($<$1%). It seems more likely that the different transcripts were generated in RNA processing. In each case, the variant mRNAs could be generated by exon skipping during splicing. It is interesting to note that as many as 30% of brain mRNAs are reported to involve exon skipping events.[21] Moreover, RNA splicing can be altered significantly in malignant cells.[22] Reciprocal fusions between the *PML* and *RARA* genes in acute promyelocytic leukemia have been shown to express several variably spliced mRNAs.[23] Thus, the presence of multiple junctions within PA_c specimens might reflect exon skipping events. The significance of this is not clear at this time.

In summary, the findings here should help to facilitate rapid and accurate analysis of pediatric low-grade astrocytomas from diverse medical institutions. Although analytic methods based on RNA extracted from FFPE tissues must be performed and interpreted with care, these assays appear reliable enough to be useful in the clinical trial setting as well as in retrospective studies that are common for these rare cancers. In light of the importance of the *KIAA1549-BRAF* fusion in the diagnosis of pilocytic tumors this test represents a feasible, cost-effective, and sensitive alternative to FISH studies to facilitate the adoption of testing for these pediatric tumors.

References

1. Louis D, Ohgaki H, Wiestler O, and Cavanese W: WHO Classification of Tumours of the Central Nervous System, 3rd ed. Edited by F Bosman, et al. Lyon, International Agency for Research on Cancer (IARC), 2007
2. Dhomen N, Marais R: New insight into BRAF mutations in cancer. Curr Opin Genet Dev 2007, 17:31–39
3. Jones DT, Kocialkowski S, Liu L, Pearson DM, Backlund LM, Ichimura K, Collins VP: Tandem duplication producing a novel oncogenic BRAF fusion gene defines the majority of pilocytic astrocytomas. Cancer Res 2008, 68:8673–8677
4. Pfister S, Janzarik WG, Remke M, Ernst A, Werft W, Becker N, Toedt G, Wittmann A, Kratz C, Olbrich H, Ahmadi R, Thieme B, Joos S, Radlwimmer B, Kulozik A, Pietsch T, Herold-Mende C, Gnekow A, Reifenberger G, Korshunov A, Scheurlen W, Omran H, Lichter P: BRAF gene duplication constitutes a mechanism of MAPK pathway activation in low-grade astrocytomas. J Clin Invest 2008, 118:1739–1749

5. Sievert AJ, Jackson EM, Gai X, Hakonarson H, Judkins AR, Resnick AC, Sutton LN, Storm PB, Shaikh TH, Biegel JA: Duplication of 7q34 in pediatric low-grade astrocytomas detected by high-density single-nucleotide polymorphism-based genotype arrays results in a novel BRAF fusion gene. Brain Pathol 2009, 19:449–458
6. Forshew T, Tatevossian RG, Lawson AR, Ma J, Neale G, Ogunkolade BW, Jones TA, Aarum J, Dalton J, Bailey S, Chaplin T, Carter RL, Gajjar A, Broniscer A, Young BD, Ellison DW, Sheer D: Activation of the ERK/MAPK pathway: a signature genetic defect in posterior fossa pilocytic astrocytomas. J Pathol 2009, 218:172–181
7. Cin H, Meyer C, Herr R, Janzarik WG, Lambert S, Jones DT, Jacob K, Benner A, Witt H, Remke M, Bender S, Falkenstein F, Van Anh TN, Olbrich H, von Deimling A, Pekrun A, Kulozik AE, Gnekow A, Scheurlen W, Witt O, Omran H, Jabado N, Collins VP, Brummer T, Marschalek R, Lichter P, Korshunov A, Pfister SM: Oncogenic FAM131B-BRAF fusion resulting from 7q34 deletion comprises an alternative mechanism of MAPK pathway activation in pilocytic astrocytoma. Acta Neuropathol 2011, 121:763–774
8. Jones DT, Kocialkowski S, Liu L, Pearson DM, Ichimura K, Collins VP: Oncogenic RAF1 rearrangement and a novel BRAF mutation as alternatives to KIAA1549: BRAF fusion in activating the MAPK pathway in pilocytic astrocytoma. Oncogene 2009, 28:2119–2123
9. Tatevossian RG, Lawson AR, Forshew T, Hindley GF, Ellison DW, Sheer D: MAPK pathway activation and the origins of pediatric low-grade astrocytomas. J Cell Physiol 2010, 222:509–514
10. Davies H, Bignell GR, Cox C, Stephens P, Edkins S, Clegg S, et al: Mutations of the BRAF gene in human cancer. Nature 2002, 417:949–954
11. Michaloglou C, Vredeveld LC, Mooi WJ, Peeper DS: BRAF(E600) in benign and malignant human tumours. Oncogene 2008, 27:877–895
12. MacConaill LE, Campbell CD, Kehoe SM, Bass AJ, Hatton C, Niu L, Davis M, Yao K, Hanna M, Mondal C, Luongo L, Emery CM, Baker AC, Philips J, Goff DJ, Fiorentino M, Rubin MA, Polyak K, Chan J, Wang Y, Fletcher JA, Santagata S, Corso G, Roviello F, Shivdasani R, Kieran MW, Ligon KL, Stiles CD, Hahn WC, Meyerson ML, Garraway LA: Profiling critical cancer gene mutations in clinical tumor samples. PLoS One 2009, 4:e7887
13. Kolb EA, Gorlick R, Houghton PJ, Morton CL, Neale G, Keir ST, Carol H, Lock R, Phelps D, Kang MH, Reynolds CP, Maris JM, Billups C, Smith MA: Initial testing (stage 1) of AZD6244 (ARRY-142886) by the Pediatric Preclinical Testing Program. Pediatr Blood Cancer 2010, 55:668–677
14. Eisenhardt AE, Olbrich H, Roring M, Janzarik W, Van Anh TN, Cin H, Remke M, Witt H, Korshunov A, Pfister SM, Omran H, Brummer T: Functional characterization of a BRAF insertion mutant associated with pilocytic astrocytoma. Int J Cancer 2010, doi: 10.1002/ijc.25893
15. Dias-Santagata D, Lam Q, Vernovsky K, Vena N, Lennerz JK, Borger DR, Batchelor TT, Ligon KL, Iafrate AJ, Ligon AH, Louis DN, Santagata S: BRAF V600E mutations are common in pleomorphic xanthoastrocytoma: diagnostic and therapeutic implications. PLoS One 2011, 6:e17948
16. Schindler G, Capper D, Meyer J, Janzarik W, Omran H, Herold-Mende C, Schmieder K, Wesseling P, Mawrin C, Hasselblatt M, Louis DN, Korshunov A, Pfister S, Hartmann C, Paulus W, Reifenberger G, von Deimling A: Analysis of BRAF V600E mutation in 1,320 nervous system tumors reveals high mutation frequencies in pleomorphic xanthoastrocytoma, ganglioglioma and extra-cerebellar pilocytic astrocytoma. Acta Neuropathol 2011, 121:397–405
17. Schiffman JD, Hodgson JG, VandenBerg SR, Flaherty P, Polley MY, Yu M, Fisher PG, Rowitch DH, Ford JM, Berger MS, Ji H, Gutmann DH, James CD: Oncogenic BRAF mutation with CDKN2A inactivation is characteristic of a subset of pediatric malignant astrocytomas. Cancer Res 2010, 70:512–519
18. Whittaker S, Menard D, Kirk R, Ogilvie L, Hedley D, Zambon A, Lopes F, Preece N, Manne H, Rana S, Lambros M, Reis-Filho JS, Marais R, Springer CJ: A novel, selective, and efficacious nanomolar pyridopyrazinone inhibitor of V600EBRAF. Cancer Res 2010, 70:8036–8044
19. Bollag G, Hirth P, Tsai J, Zhang J, Ibrahim PN, Cho H, et al: Clinical efficacy of a RAF inhibitor needs broad target blockade in BRAF-mutant melanoma. Nature 2010, 467:596–599
20. Holland PM, Abramson RD, Watson R, Gelfand DH: Detection of specific polymerase chain reaction product by utilizing the 5′–3′ exonuclease activity of Thermus aquaticus DNA polymerase. Proc Natl Acad Sci U S A 1991, 88:7276–7280
21. Yeo G, Holste D, Kreiman G, Burge CB: Variation in alternative splicing across human tissues. Genome Biol 2004, 5:R74
22. Ghigna C, Valacca C, Biamonti G: Alternative splicing and tumor progression. Curr Genomics 2008, 9:556–570
23. Jensen K, Shiels C, Freemont PS: PML protein isoforms and the RBCC/TRIM motif. Oncogene 2001, 20:7223–7233